Aerosol and Air Quality Research, 17: 2751–2761, 2017

ISSN: 1680-8584 print / 2071-1409 online
doi: 10.4209/aaqr.2017.06.0213

Influence of Long-Range Transport of Siberian Biomass Burning at the Mt. Bachelor Observatory during the Spring of 2015

Pao Baylon[1,2*], Daniel A. Jaffe[1,2], Joost de Gouw[3], Carsten Warneke[3]

[1] *Department of Atmospheric Sciences, University of Washington, Seattle, Washington 98195, USA*
[2] *School of Science, Technology, Engineering and Mathematics, University of Washington Bothell, Bothell, Washington 98011, USA*
[3] *NOAA Earth System Research Laboratory, Boulder, CO 80305, USA*

ABSTRACT

We looked at a Siberian biomass burning (BB) event on Spring 2015 that was observed at Mt. Bachelor Observatory (MBO; 2.8 km a.s.l) and by satellite instruments (MODIS and CALIPSO), and intercepted by the NOAA WP-3D research aircraft during the Shale Oil and Natural Gas Nexus (SONGNEX) campaign. The Siberian airmass split into two plumes in the eastern Pacific. One plume moved eastward and was sampled directly at MBO. The other moved northeast to Alaska and then down to the U.S. Midwest; this second plume was intercepted by the WP-3D aircraft. We find that the $\Delta O_3/\Delta CO$ enhancement ratio at MBO is higher than for the plume intercepted by the aircraft. This is due to the warmer plume observed at MBO which led to thermal decomposition of PAN to NO_x. The colder plume observed by the aircraft allowed PAN to be locked up and therefore this led to less ozone production. This is supported by the reactive nitrogen (NO_y) measurements from the aircraft, which show that 64% of the NO_y is stored as PAN. We also find that the $\Delta\sigma_{sp}/\Delta CO$ enhancement ratios at MBO and on the aircraft were much higher than the ratios for similarly aged Siberian fires that were observed previously in the western U.S. We observe that this is because of dust transport in addition to the fire smoke. Ground-based, satellite, and LiDAR data suggest that the Siberian plume was transported at high elevation, and while it was efficiently transported across the Pacific, there was no significant subsidence over North America. Therefore, this long-range transport event did not lead to air quality impacts at the surface in western North America.

Keywords: Ozone; Wildfire plumes; Mountaintop sites; Aircraft; Reactive nitrogen; Aerosol.

INTRODUCTION

Biomass burning (BB) is a significant source of trace gases (i.e., CO, NO_x, VOCs) and particulate matter (PM) in the atmosphere (Crutzen and Andreae, 1990; Andreae, 1991; Andreae and Merlet, 2001; Real *et al*., 2007; Martins *et al*., 2012). These emissions lead to the formation of secondary pollutants with consequences ranging from local to global in scale. One of these secondary pollutants is ozone, which forms in the troposphere from the interaction of nitrogen oxides ($NO_x = NO + NO_2$) and volatile organic compounds (VOCs) in the presence of sunlight (Finlayson-Pitts and Pitts, 2000). Ozone is a health hazard to sensitive individuals (Bell *et al.*, 2006), is the third strongest anthropogenic greenhouse gas (Henderson *et al*., 2012), and is the main source of hydroxyl radicals that drive the oxidizing capacity of the atmosphere (Seinfeld and Pandis, 1998; Monks *et al.*, 2009). Moreover, it damages food crops, forests, and other ecosystems (Fiscus *et al*., 2005).

The rate of ozone formation in wildfire plumes is complicated by various factors (Akagi *et al*., 2011). While Jaffe and Wigder (2012) broadly showed in their review paper that the $\Delta O_3/\Delta CO$ enhancement ratio, which was used as a measure of ozone production, generally increases with plume age, they note that there is a lot of variability. Uncertainties such as fire emissions, combustion efficiency, meteorological patterns, chemical and photochemical reactions, aerosol effects on chemistry, and solar radiation complicate quantifying ozone production from wildfires. More studies are needed to investigate the impact of fires on downwind air quality for long-range transport (LRT) events.

Total reactive nitrogen is represented by NO_y ($NO + NO_2 + HNO_3 + PAN + HONO + NO_3 + N_2O_5$ + aerosol nitrate + …). Peroxyacetyl nitrate (PAN) is an important reservoir of NO_x in the atmosphere. It can be transported over long distances and can thermally decompose back to NO_x as the plume descends to warmer temperatures (Jacob,

* Corresponding author.
Tel.: 1-425-312-9155
E-mail address: paolo.baylon@gmail.com

1999; Kotchenruther *et al*., 2001). Later, this NO_x could be involved again in O_3 production. Therefore, NO_y speciation can provide insights about O_3 production from BB plumes.

It is well established that Asian long-range transport (ALRT) episodes, which can be natural (i.e., biomass burning) or anthropogenic (i.e., fossil fuel burning, biofuel burning, human-caused fires), contain trace gases and particulates such as ozone, CO, NO_x, VOCs, and dust that can be transported across the Pacific under certain meteorological conditions (Jaffe *et al*., 1999; Liang *et al*., 2004; Teakles *et al*., 2017). Siberian BB events during the summer of 2003 resulted in ozone and CO enhancements from the background of 5–9 ppbv and 23–37 ppbv, respectively, at 10 surface stations in Alaska, Canada and the Pacific Northwest, contributing to exceedances in the national air quality standards (Jaffe *et al*., 2004). In another large event, ozone and CO exceeded 100 ppbv and 220 ppbv, respectively (Bertschi and Jaffe, 2005). Similarly, the Siberian fires in July 2012 resulted in trans-Pacific transport of a large smoke plume which affected air quality in British Columbia and Washington State (Teakles *et al*., 2017). Ozone and $PM_{2.5}$ enhancements of 34–44 ppbv and 10–32 μg m^{-3}, respectively, were observed. Smaller ozone and $PM_{2.5}$ enhancements of 10 ppbv and 4–9 μg m^{-3} were observed at sites with stable atmospheric conditions, leading to stagnant conditions which limited the entrainment of the fire plume into the boundary layer (BL) (Teakles *et al*., 2017). $\Delta O_3/\Delta CO$ enhancement ratios for the Siberian 2012 BB events observed at Whistler high-elevation site had a mean value of 0.26 ppbv/ppbv, comparable to other similarly aged Siberian wildfire plumes with ratios of 0.22–0.36 ppbv/ppbv (Bertschi *et al*., 2005) and 0.15–0.84 ppbv/ppbv (Bertschi and Jaffe, 2005). Recently, Laing *et al*. (2016) looked at Siberian plumes transported to the western U.S. during the summer of 2015. The transport of BB plumes and anthropogenic pollution from China and Russia to Japan is also well-studied (Zhu *et al*., 2015a, b).

These studies suggest that long-range transport of Siberian BB emissions has far-reaching impacts on surface air quality downwind. However, air quality impacts can vary with downwind meteorology and entrainment pathways. Smaller ozone and PM enhancements at the surface are associated with stable atmospheric conditions and BL transport. On the other hand, higher enhancements are linked to free tropospheric (FT) transport, strong source, and favorable transport.

Aerosol scattering (σ_{sp}) is wavelength-dependent (Ångström, 1929). This relationship is parameterized in terms of the scattering Ångström exponent ($Å_s$). For large particles such as dust, σ_{sp} changes little with wavelength, so $Å_s$ is small. For small particles such as those emitted directly from combustion, σ_{sp} decreases rapidly with wavelength, so $Å_s$ is large.

The Mt. Bachelor Observatory (MBO; 2.8 km a.s.l.) is a mountaintop site established by the University of Washington Atmospheric Chemistry group in 2004 (Jaffe *et al*., 2005). Data from MBO has been extensively used to study the LRT of natural and anthropogenic pollution from Siberia and Asia to North America. Year-to-year variability of ALRT events observed at MBO can be traced to variability in both emission source and transport (Reidmiller *et al*., 2009).

In this paper, we examine an episodic LRT of Siberian wildfire smoke to the western U.S. on April 2015. We use FT data from MBO and from the NOAA WP-3D research aircraft during the Shale Oil and Natural Gas Nexus (SONGNEX) campaign, as one of these flights intercepted the Siberian plume. We also look at BL sites in the western U.S. We are interested in answering the following questions:

- Were the MBO and aircraft observations consistent with respect to the enhancement ratios?
- What caused the relatively high $\Delta O_3/\Delta CO$ and $\Delta\sigma_{sp}/\Delta CO$ ratios for the Siberian 2015 fires?
- Was there O_3 production and if so, was this O_3 mixed into the boundary layer? Was there entrainment from the upper troposphere/lower stratosphere (UT/LS)?
- How does the reactive nitrogen speciation of the plume relate to O_3 production?

METHODS

Mt. Bachelor Observatory (MBO) is a mountaintop site established in 2004 (Jaffe *et al*., 2005). It is located on the summit of Mt. Bachelor in the Cascades Mountains of central Oregon. Mt. Bachelor is located in the Deschutes National Forest and is home to a ski resort. Measurements of σ_{sp} (TSI Model 3563), O_3 (Dasibi 1008 RS) and CO (May 2012 onwards: Picarro G2302), along with measurements of basic meteorology, such as temperature, humidity and wind speed, have been on-going at MBO since 2004 (see Ambrose *et al*., 2011 and Gratz *et al*., 2014 and references therein for details on σ_{sp}, O_3 and CO instrumentation).

We also used measurements from the NOAA WP-3D Orion research aircraft during the Shale Oil and Natural Gas Nexus (SONGNEX) campaign in Spring 2015. The mission of SONGNEX was to quantify atmospheric emissions from various U.S. energy infrastructures and to study how these emissions transform chemically in the atmosphere and how they contribute to ozone and PM formation (https://esrl.noaa.gov/csd/projects/songnex/). The NOAA WP-3D aircraft was based in Broomfield, CO, and Austin, TX. Twenty research flights were conducted between March 19 and April 27, 2015 over oil and gas production regions in the western U.S. The aircraft was equipped with an extensive set of gas-phase measurements, including instruments for methane, CO, canister samples for VOCs, NO_x, NO_y, PAN, and ozone. NO_x, NO_y, and O_3 were measured using chemiluminescence detection with photolytic or catalytic conversion. PAN and HNO_3 were measured using chemical ionization mass spectrometry with I^- as reagent ion. CO was measured using vacuum UV resonance fluorescence. Aerosol scattering coefficient (σ_{sp}) at 532 nm was calculated from the ultrahigh sensitivity aerosol size spectrometer (UHSAS) size distribution. One of the SONGNEX flights sampled the Siberian plume. This gives us an opportunity to study a similar, possibly the same, plume at both MBO and via the aircraft.

Observations of O_3 in Boise City, ID (air quality system

identification: 16-001-0010); Idaho Falls, ID (16-023-0101); and Portland, OR (41-067-0005) were obtained from the U.S. EPA AirData archive (www.epa.gov/airdata). Fig. 1 shows a map of the surface sites and the aircraft flight track. We also used V3.30 aerosol classification products from the Cloud-Aerosol Lidar with Orthogonal Polarization (CALIOP) instrument on the Cloud-Aerosol Lidar Infrared Pathfinder Satellite Observation (CALIPSO) satellite to confirm the transport of smoke from Siberia to the western U.S. (https://www-calipso.larc.nasa.gov). We ran the HYSPLIT (Hybrid Single Particle Lagrangian Integrated Trajectory Model) backtrajectories and forward dispersion to identify the transport time and mechanisms (http://ready.arl.noaa.gov/HYSPLIT.php). HYSPLIT links to the Air Resources Laboratory (ARL) and National Weather Service (NWS) meteorological data server. Finally, we used the Navy Aerosol Analysis and Prediction System (NAAPS) Global Aerosol Model (https://www.nrlmry.navy.mil/aerosol/) to look at the forecast total optical depth and smoke surface concentrations. NAAPS presents optical depth at a wavelength of 550 nm for three components: sulfate, dust, and smoke.

RESULTS AND DISCUSSION

Siberian 2015 Smoke Event Overview

In April 2015, huge agricultural fires burned in the steppes of southern Russia, on the outskirts of the city of Chita. These fires are routinely set to fertilize the soil for the coming year, but abnormally warm temperatures and strong winds in April 2015 led to out-of-control fires that burned several villages and killed dozens of people (https://earthobservatory.nasa.gov/NaturalHazards//view.php?id=85707). Fig. S1 shows a true-color image of the Zabaikalsky Territory on April 14, 2015 from the Moderate Resolution Imaging Spectroradiometer (MODIS) aboard NASA's Terra satellite. Active burning locations are outlined in red. Smoky air is evident throughout the region. Typically, these fires remain in the BL. However, because of unusually warm temperatures and a baroclinic cyclone that developed near Chita, Russia, they were lofted high up into the upper troposphere where strong upper-level winds rapidly transported the smoke plume. Fig. S2 shows both a MODIS infrared (IR) image from NASA's Aqua satellite and a Lidar image from the CALIOP instrument on the CALIPSO satellite. Both were taken overnight on April 15, 2015. The Lidar image shows the vertical profile for the red line in the top figure which represents the north-south flight of the CALIPSO satellite (overpass at the Sea of Okhotsk). CALIOP detected smoke between 4–10 kilometers (2–6 miles). This height indicates that the smoke plumes were injected relatively high in the atmosphere.

It is well-established that Asian dust can be transported across the Pacific during springtime (Jaffe *et al.*, 2003; Fischer *et al.*, 2010). Therefore, it is possible that the Siberian BB plume is mixed with dust.

After the Siberian smoke was lofted high in the atmosphere, strong upper-level winds carried it over the Sea of Okhotsk and eventually across the Pacific Ocean. Fig. S3 shows a true-color MODIS image of the smoke moving across the Pacific into the west coast of North America on April 18, 2015.

Fig. S4 shows Terra MODIS images over the Pacific Northwest from April 17–19, 2015. Fig. S5 shows the Lidar image from CALIPSO on April 19, 2015. At this time, Siberian fires were observed at an elevation of 4–8 kilometers, consistent with the initial observed heights at the source described in Fig. S2.

Siberian Plume Observations in the FT at MBO

At MBO, we observed hourly aerosol scattering (550 nm) values of ~130 Mm^{-1} (this amounts to a PM mass concentration of ~43 $\mu g\ m^{-3}$) and hourly ozone of ~85 ppbv on April 21, 2015 (Fig. 2). Water vapor during these PM and O_3 peaks was ~0.9 $g\ kg^{-1}$, which is characteristic of dry, FT air. Fig. 3 shows plots of hourly ozone, water vapor, CO, and σ_{sp} (550 nm) observed at MBO for the entire month of April 2015. The period from April 20–21 stands out because of the high ozone, CO, and σ_{sp}, and low water vapor observed at MBO.

To verify the influence of Siberian smoke on our MBO observations, we perform a 10-day HYSPLIT backtrajectory

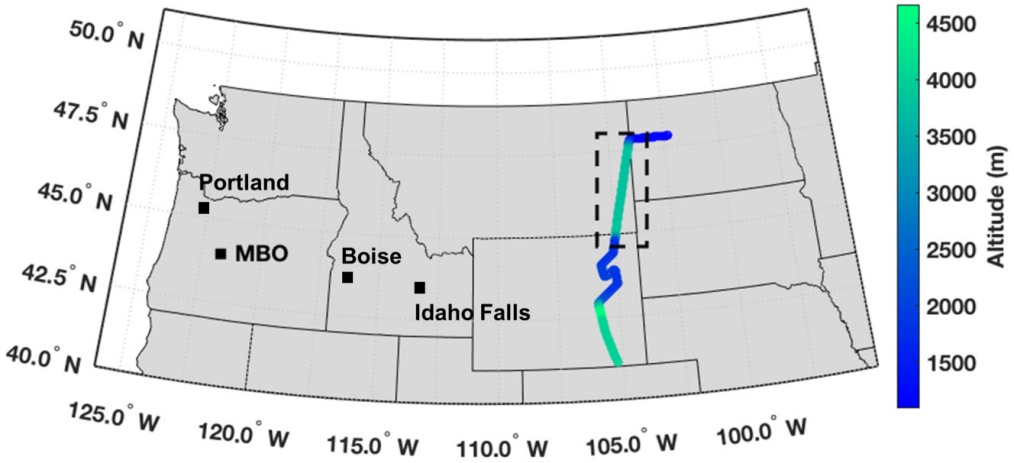

Fig. 1. Location of air quality sites used in this study and the flight track of SONGNEX on 21 April 2015.

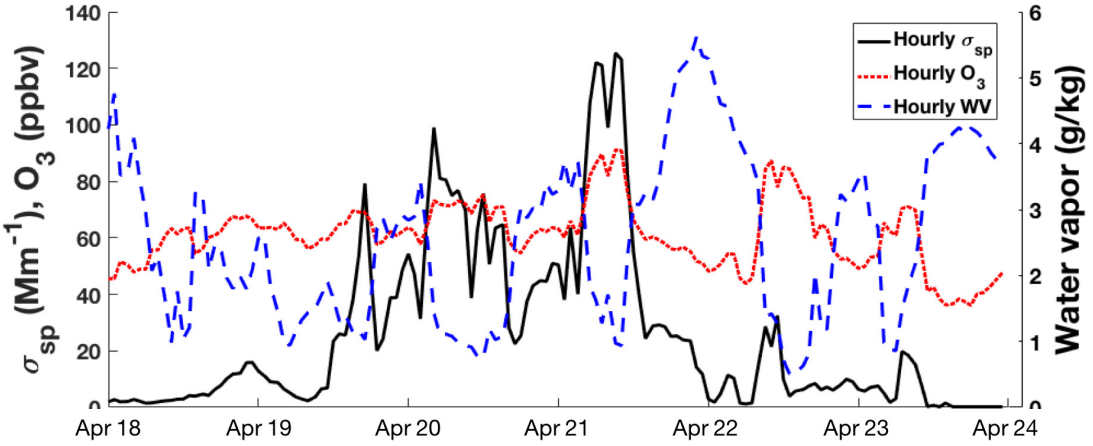

Fig. 2. Time series of hourly σ_{sp}, O_3, and water vapor at MBO during the Siberian smoke observation.

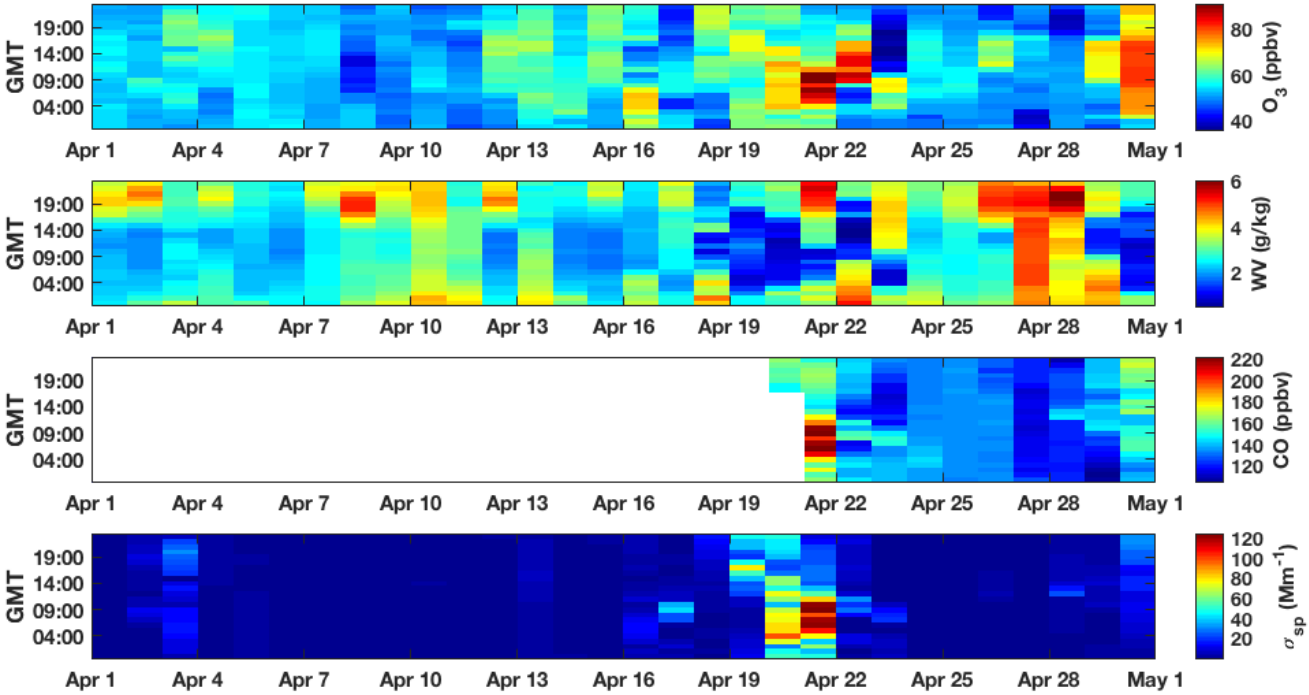

Fig. 3. Plots of hourly O_3, water vapor, CO, and σ_{sp} observed at MBO on April 2015.

(Figs. 4(a)–4(f)). Results confirm that the pollution episode came from Siberia and that the plume stayed in the FT for the most part during its transport. Wet deposition was minimal as indicated by the negligible rainfall (Fig. 4(c)). Relative humidity was also low during transport (Fig. 4(d)). We now look at the observations from the NOAA WP-3D aircraft.

Siberian Plume Observations in the FT on the NOAA WP-3D Research Aircraft

One of the flights during the SONGNEX field campaign in 2015 also intercepted the Siberian plume on April 21. Fig. 1 shows the location of the flight track with respect to the location of MBO. Fig. 5 shows a time series of the CO, σ_{sp}, and O_3 data from the aircraft. We divide the aircraft (AC) time series into three (AC plumes 1, 2, and 3) because the ozone-CO plots for these three plumes appear distinct from each other (Fig. 7(a)). From 22:30–22:39 UTC (Fig. 5(b)), the aircraft intercepted a plume (AC plume 1) with elevated CO, σ_{sp}, and O_3 levels. From 22:39–22:42 UTC (Fig. 5(c)), a similar plume (AC plume 2) with higher O_3 levels was observed. However, from 22:42–22:52 UTC (Fig. 5(d)), the aircraft intercepted a plume that was rich in ozone but relatively lower in CO (AC plume 3).

Hourly CO and ozone at MBO on April 21 09:00 UTC were 223 ppbv and 91.1 ppbv, respectively. On the other hand, instantaneous CO and ozone measurements from the aircraft on April 21 during the plume intercept (~22:28–22:40 UTC) ranged from 200-300 ppbv and 70-85 ppbv, respectively. The CO observed by the aircraft is comparable to the measurements at MBO. However, the ozone observed by the aircraft is lower than that observed in MBO. The MBO

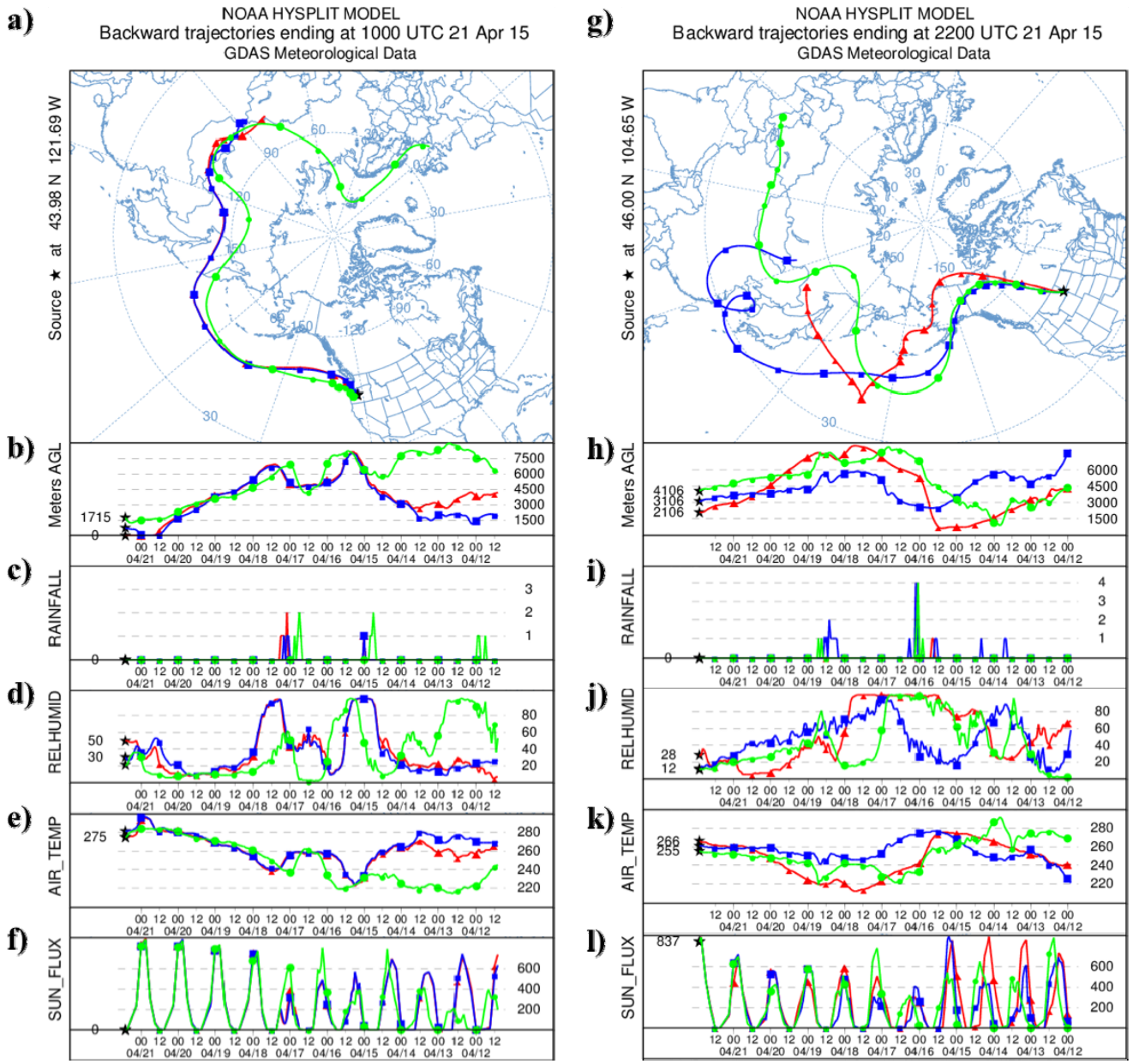

Fig. 4. Ten-day HYSPLIT backtrajectories initiated (a–f) at MBO and (g–l) at the location of the aircraft. Red, blue, and green lines represent backtrajectories initiated at three different heights: 1000, 2000, and 3000 meters a.s.l. for MBO; and 3000, 4000, and 5000 meters a.s.l. for the aircraft. Also plotted are the rainfall (in mm hr^{-1}), relative humidity (%), air temperature (in K), and downward solar radiation (in W m^{-2}) values from the meteorological fields used for the trajectories. Consecutive trajectory points are 12 hours apart.

and aircraft observations are 13 hours apart. We perform HYSPLIT forward dispersion runs initiated at MBO (April 21 09:00 UTC) and observe that it takes ~70 hours for a plume to be transported from MBO to the location of the aircraft. Fig. S6 shows the time-of-arrival plot. Given that the MBO and the SONGNEX aircraft observed this plume only 13 hours apart, this indicates that the Siberian plume observed at MBO on 09:00 UTC was not the same plume intercepted by the aircraft at ~22:28 UTC, but was of similar Siberian origin.

To identify the origin of the plume intercepted by the aircraft, we look at the Global Aerosol Model from the Navy Aerosol Analysis and Prediction System (NAAPS) (Figs. 6 and S7) and HYSPLIT backtrajectories (Figs. 4(g)–4(l)). We find from the total aerosol optical depth (AOD) plots in Fig. S7 that as the Siberian plume crossed the eastern Pacific, it splits (note that green/yellow shading represents dust while blue shading represents smoke): one plume moves eastward and the other moves over Alaska and down to the U.S. mid-West. MBO observed the former while the aircraft intercepted the latter. Both plumes are Siberian in origin but were transported through different pathways. Fig. 6 shows the NAAPS AOD forecast on April 22, 2015 at 00:00Z.

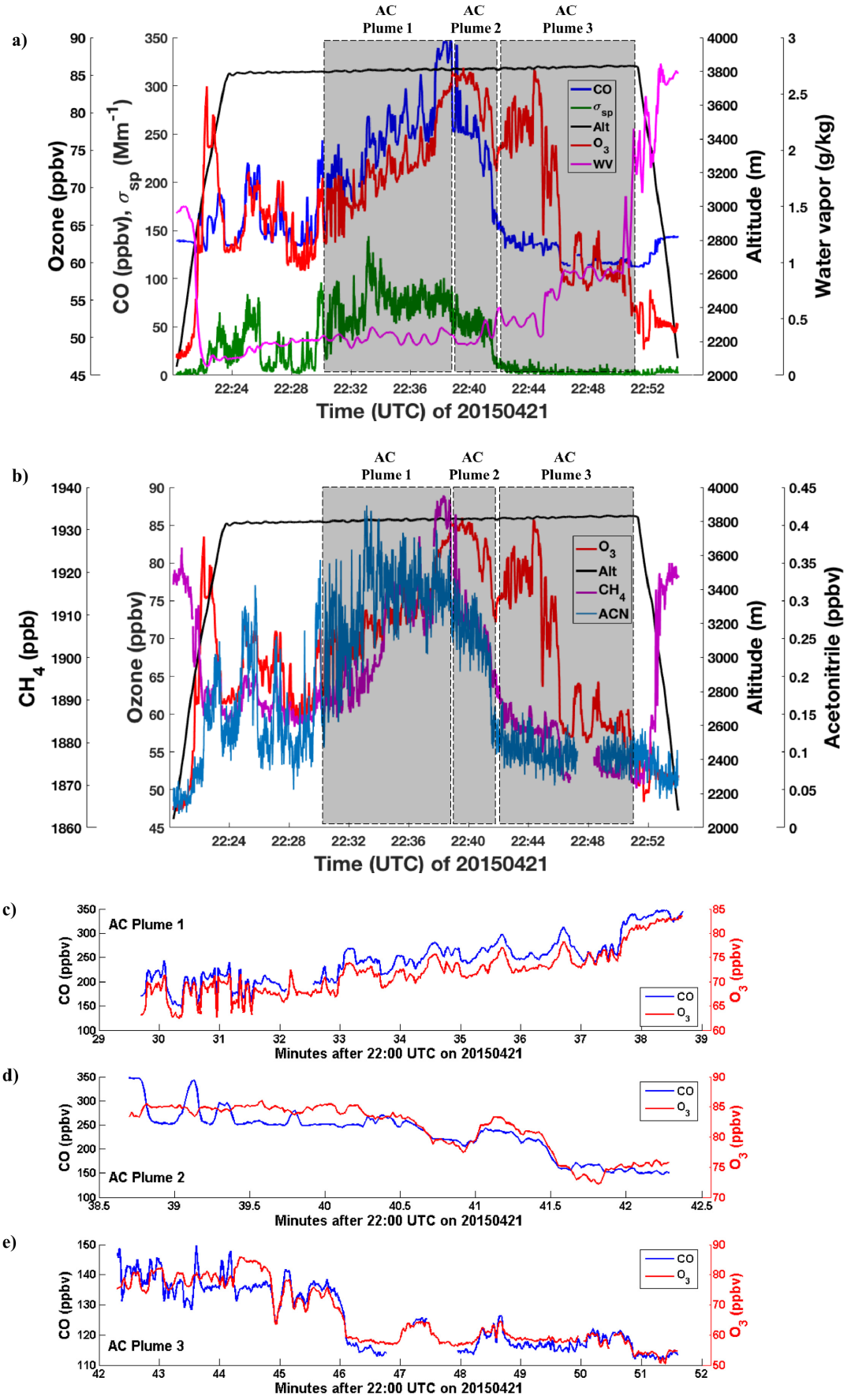

Fig. 5. Aircraft data during the April 21 flight.

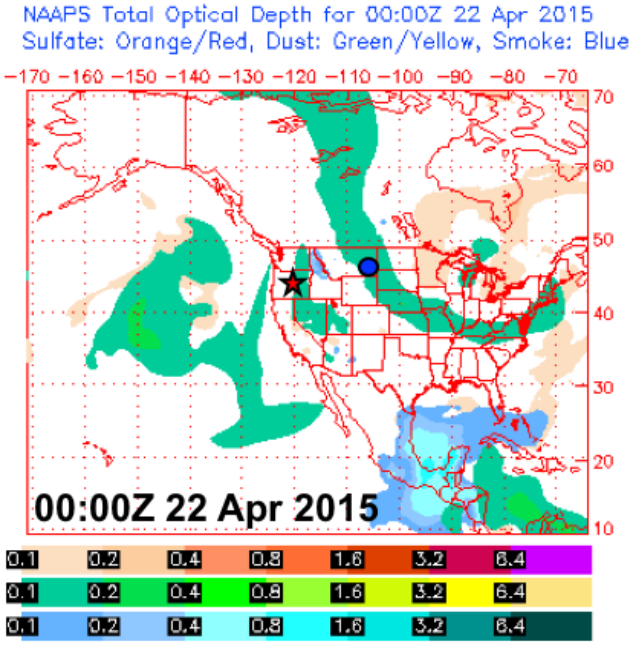

Fig. 6. AOD forecast from the Global Aerosol Model of the Navy Aerosol Analysis and Prediction System (NAAPS). The location of MBO and the NOAA WP-3D aircraft are represented by the red star and blue circle, respectively.

Figs. 4(g)–4(l) show HYSPLIT backtrajectories initiated at the location of the aircraft. Compared to the backtrajectories initiated at MBO (Figs. 4(a)–4(f)), the backtrajectories corresponding to the aircraft data suggest that the plume encountered more hours in rainfall (Fig. 4(i)) and higher relative humidity (Fig. 4(j)). This could lead to aerosol deposition, which could explain why the aircraft observed lower $\Delta\sigma_{sp}/\Delta CO$ ratios than at MBO (Table 1).

Enhancement Ratios of the Siberian Plume

We now look at scatter plots of O_3, σ_{sp}, and NO_y with respect to CO (Fig. 7). From the scatter plots of multiple measurements of Y plotted against X, we can calculate the enhancement ratio ($\Delta Y/\Delta X$) by taking the slope of a Reduced Major Axis (RMA) linear regression. A comparison of different approaches to get the enhancement ratio is shown in the paper by Briggs *et al*. (2016). These enhancement ratios, along with results from similarly aged Siberian plumes observed in North America, are summarized in Table 1. Bertschi *et al*. (2004) reported plume heights from 1–4 km whereas Teakles *et al*. (2017) reported heights from 2–3.6 km. The Siberian 2015 fires were transported at higher elevations (4–10 km). Note that NO_y was not measured at MBO during Spring 2015. Because CO data at MBO was available only on April 21, we calculate these ratios at MBO for this day only. All three parameters are well-correlated. $\Delta O_3/\Delta CO$ is 0.455 ppbv/ppbv ($R^2 = 0.90$) and $\Delta\sigma_{sp}/\Delta CO$ enhancement ratio is 1.83 Mm^{-1}/ppbv ($R^2 = 0.92$) at MBO.

The aircraft intercepted plumes with three distinct O_3-CO profiles. The first two plumes (AC plumes 1 and 2) had $\Delta O_3/\Delta CO$ enhancement ratios of 0.10 and 0.084 ppbv/ppbv which are lower than, but within the bounds of, the values from other studies (Table 1). During the latter part of the plume crossing (AC plume 3), the aircraft intercepted an ozone-rich airmass that had lower CO levels (Fig. 5(a)), but still with a strong, positive O_3-CO correlation, with an $\Delta O_3/\Delta CO$ enhancement ratio of 0.97 ppbv/ppbv, much higher than AC plumes 1 and 2. This high value is mostly driven by the lower CO enhancement. We hypothesize that AC plume 3 could be mixed with non-BB air (low acetonitrile values in Fig. 5(b); acetonitrile is a BB tracer (Bange and Williams, 2000; Palmer *et al*., 2013; Parrington *et al*., 2013)), probably from a local pollution source as evidenced by the increasing water vapor during the plume crossing (Fig. 5(a)). Upper troposphere/lower stratosphere (UT/LS) air is not likely a dominant factor as this type of air is typically associated with negatively correlated O_3 and CO profiles (Ambrose *et al*., 2011). Fig. 5(e) shows that O_3 and CO are well-correlated for AC plume 3. However, the methane concentrations for AC plume 3 are low, which could suggest some UT/LS influence. Overall, it appears that AC plume 3 is likely a mix of sources.

The $\Delta O_3/\Delta CO$ ratio at MBO is higher than AC plumes 1 and 2 and this could be explained by more subsidence in the Siberian plume arriving at MBO (Fig. 4(b)) and less subsidence for the aircraft observations (Fig. 4(h)). The plume was warmer at MBO (275 K). At this temperature, PAN has a lifetime of 1.5 days. Given that the plume stayed at this temperature for 2 days prior to being sampled at MBO (Fig. 4(e)), PAN must have decomposed back to NO_x which then led to ozone production, hence the higher $\Delta O_3/\Delta CO$ ratio at MBO. On the other hand, the aircraft observations were colder (255–260 K) (Fig. 4(k)). At these temperatures, PAN has a lifetime of 27–77 days. This suggests that NO_x remained locked up as PAN during transport and did not lead to ozone production, hence the lower $\Delta O_3/\Delta CO$ ratios for the aircraft data.

For the $\Delta\sigma_{sp}/\Delta CO$ ratios summarized in Table 1, two things stand out. First, the $\Delta\sigma_{sp}/\Delta CO$ ratios at MBO are five times larger than the ratios for all three AC plumes. This is because of the different transport mechanisms for both observation platforms. Fig. 4 shows that the transport time back to the smoke region is 6 days for MBO and 10 days for the AC. Moreover, Fig. 4 suggests that the AC trajectories were exposed to more hours in rainfall (cumulative rainfall rate of 11 mm hr^{-1} for the AC and only 5 mm hr^{-1} for MBO) and more hours with high relative humidity (6 trajectory points for the AC with relative humidity > 90% and only 2 for MBO). Overall, these backtrajectories suggest more washout for the AC transport, which is consistent with the lower $\Delta\sigma_{sp}/\Delta CO$ ratios compared to MBO.

Second, the $\Delta\sigma_{sp}/\Delta CO$ ratios for the Siberian 2015 fire plumes are on the higher end of the observed ratios in similarly aged plumes (Table 1). In particular, the $\Delta\sigma_{sp}/\Delta CO$ ratio at MBO is the highest among any observed plumes. Based on emission factors for biomass burning reported by Akagi *et al*. (2011), crop residue and boreal fires have a $\Delta PM/\Delta CO$ emission factor ratio of 0.06 ± 0.03 μg m^{-3} and 0.12 ± 0.06 μg m^{-3}, respectively. The corresponding $\Delta PM/\Delta CO$ ratios at MBO and AC plumes 1, 2, and 3 are

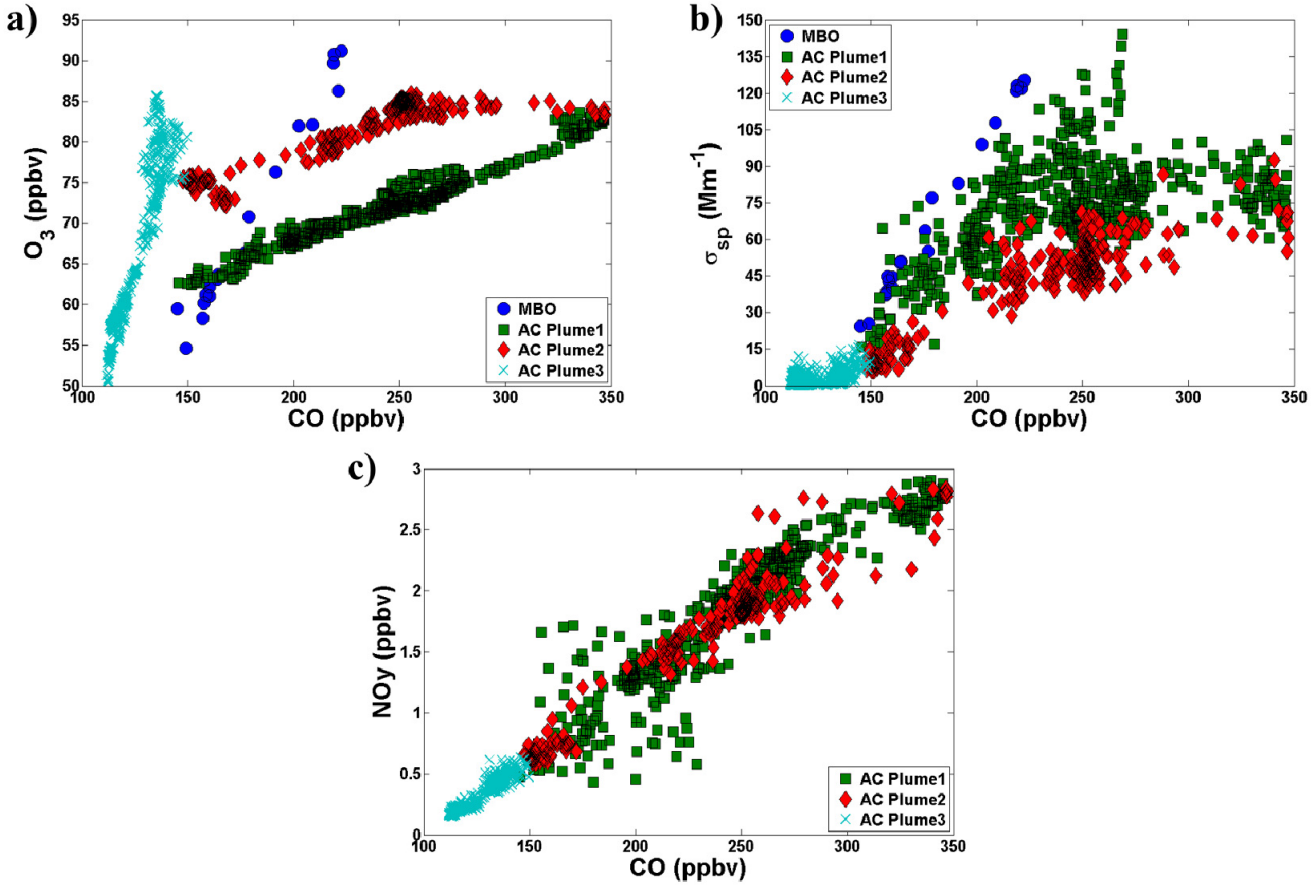

Fig. 7. Scatter plots of (a) O_3, (b) σ_{sp}, and (c) NO_y with respect to CO for both aircraft and MBO data.

Table 1. $\Delta O_3/\Delta CO$, $\Delta\sigma_{sp}/\Delta CO$, and $\Delta NO_y/\Delta CO$ ratios for similarly aged Siberian plumes observed in North America, and for the Siberian 2015 plume observed at MBO and on the NOAA WP-3D aircraft (AC) during the SONGNEX campaign. All ratios with σ_{sp} are reported relative to STP (standard temperature and pressure). σ_{sp} data from the SONGNEX aircraft are calculated from size distributions, not directly measured.

	Reference	$\Delta O_3/\Delta CO$ (ppbv/ppbv)	$\Delta\sigma_{sp}/\Delta CO$ (Mm^{-1}/ppbv)	$\Delta NO_y/\Delta CO$ (ppbv/ppbv)
Spring 2002	Bertschi *et al.* (2004)	0.22–0.42	0.27–0.88	-
Summer 2003	Jaffe *et al.* (2004)	0.14–0.39	-	-
Summer 2012	Teakles *et al.* (2017)	0.26	0.24	-
Spring 2015 (This study)	MBO	0.46	1.83	-
	AC Plume 1	0.1	0.42	0.0124
	AC Plume 2	0.084	0.4	0.0119
	AC Plume 3	0.97	0.31	0.0123

0.61, 0.14, 0.13, and 0.10 μg m^{-3}, respectively. The higher ratios for the Siberian 2015 fires suggest an additional source aside from the BB smoke. AOD forecasts from NAAPS (Figs. 6 and S7) confirm that this additional PM comes from dust (green/yellow shade). The calculated scattering Ångström exponent for this event at MBO (using the 450–700 nm pair) is 1.9, which is indicative of a smoke/dust mixture.

Despite the differences in the ratios of both $\Delta O_3/\Delta CO$ (Fig. 7(a)) and $\Delta\sigma_{sp}/\Delta CO$ (Fig. 7(b)) across AC plumes 1, 2, and 3, the NOy-CO profiles for all three plumes lie on the same line (Fig. 7(c)). The slopes are identical (Table 1). This provides us insights about the total reactive nitrogen budget in long-range transported BB smoke.

All other events enumerated in Table 1 reported effects on surface air quality via ozone exceedances. Later, we look at effects of the Siberian 2015 fires on surface air quality in the western U.S.

Fig. 8 shows a time series of the reactive nitrogen species in the Siberian plume observed by the aircraft. Most of the NO_y (64%) is stored as PAN. NO_x is insignificant (3.3%). This suggests that most photochemical production of O_3 from the plume likely has not happened. However, if the plume warmed up (i.e., via descent), then PAN would

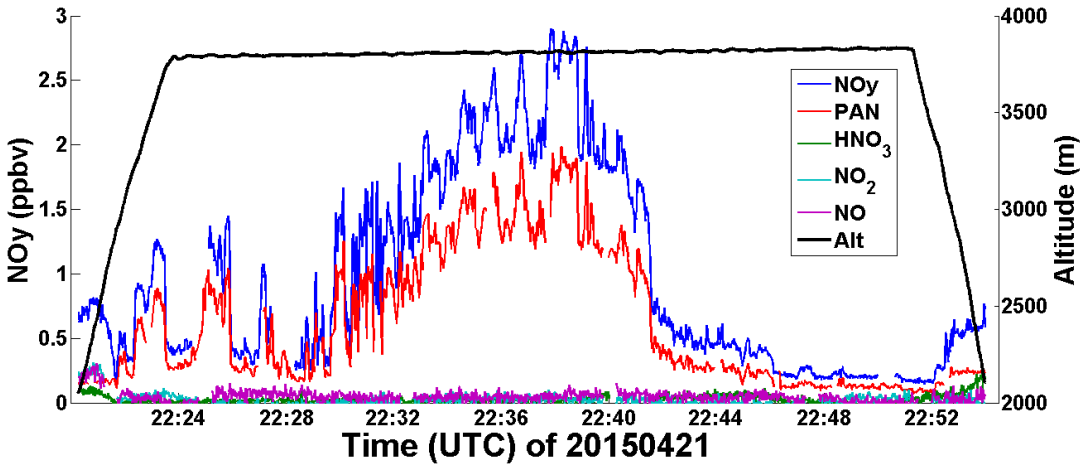

Fig. 8. NO_y speciation of the plume observed by the aircraft.

decompose back to NO_x and ozone formation can take place. For comparison, Briggs *et al*. (2016) looked at regional fires observed at MBO during summer 2012 and 2013 and found that PAN comprised 25–57% of the total reactive nitrogen. Table S1 quantifies the reactive nitrogen speciation for AC plumes 1, 2, and 3.

Siberian Plume Observations in the BL

Finally, we pick sites in the Pacific Northwest that have data on April 2015. We focus on Oregon and Idaho as these states are the most impacted by the Siberian plumes based on the MODIS images (Figs. S3 and S4). Aside from MBO, we selected Boise (826 m a.s.l.), Idaho Falls (1815 m), and Portland (53 m) (see Fig. 1). Fig. S8 shows a time series of the maximum daily average 8–hour (MDA8) ozone at these sites for April 2015. MBO has the highest MDA8 values (50–85 ppbv) compared to the other sites. Idaho Falls showed a small enhancement but no other sites showed a similar trend. This supports the satellite and Lidar observations that most of the Siberian smoke has stayed aloft.

CONCLUSIONS

In April 2015, huge agricultural fires burned in the steppes of Southern Russia. Due to strong winds, the fires burned out of control and likely mobilized large amounts of mineral dust as well. The smoke and dust were injected relatively high in the atmosphere where strong upper-level winds dispersed them widely. We used data at Mt. Bachelor Observatory in central Oregon (MBO; 2.8 km a.s.l.) and from the NOAA WP-3D aircraft during the Shale Oil and Natural Gas Nexus (SONGNEX) campaign to examine the plume chemistry downwind of the fire source. We find that both platforms observed a plume of Siberian origin but not the same exact plume.

We find that $\Delta O_3/\Delta CO$ enhancement ratio at MBO is higher than for the plume intercepted by the aircraft. This is due to the warmer plume observed at MBO which led to thermal decomposition of PAN to NO_x. The colder plume observed by the aircraft allowed PAN to be locked up and therefore this led to less ozone production. We also find that the $\Delta\sigma_{sp}/\Delta CO$ enhancement ratios at MBO and on the aircraft were much higher than the ratios for similarly aged Siberian fires that were observed previously in the western U.S. We observe that this is because of dust transport in addition to the smoke. We also hypothesize minimal wet scavenging of aerosols en route to MBO because of the relatively intact nature of the Siberian plume. For the aircraft, greater plume encounter with clouds reduced the aerosol loading. We also observe that 64% of the reactive nitrogen in the Siberian plume intercepted by the aircraft is in the form of PAN and that NO_x was a minor component of the plume. This suggests that most photochemical production of ozone from this part of the plume has not happened, but can occur once the plume warms up during descent. The Siberian 2015 fires that we studied did not lead to air quality enhancements at the surface in North America. This is because the Siberian fires were lofted at 4–10 kilometers a.s.l. in Russia, and while the plumes were efficiently transported across the Pacific, there was no significant high-pressure system to cause subsidence and mixing into the boundary layer.

ACKNOWLEDGMENTS

The authors thank Jonathan Hee for finalizing the datasets at MBO. We also thank the MBO staff for their support and assistance. We acknowledge Charles Brock for the aerosol scattering data; John Holloway for the CO data; Tom Ryerson for the ozone and NO_y data; Patrick Veres for the PAN data; Andy Neuman for the HNO_3 data; and Robert Wild for the NO_x data collected during the SONGNEX campaign. The authors gratefully acknowledge the NOAA Air Resources Laboratory (ARL) for the provision of the HYSPLIT transport and dispersion model and/or READY website (http://www.ready.noaa.gov) used in this publication. The CALIPSO satellite products were supplied from the NASA Langley Research Center. Funding for research at MBO was supported by the National Science Foundation (grant number: 1447832) and the NOAA Earth System Research Laboratory.

SUPPLEMENTARY MATERIAL

Supplementary data associated with this article can be found in the online version at http://www.aaqr.org.

REFERENCES

Akagi, S.K., Yokelson, R.J., Wiedinmyer, C., Alvarado, M.J., Reid, J.S., Karl, T., Crounse, J.D. and Wennberg, P.O. (2011). Emission factors for open and domestic biomass burning for use in atmospheric models. *Atmos. Chem. Phys*. 11: 4039–4072.

Ambrose, J.L., Reidmiller, D.R. and Jaffe, D.A. (2011). Causes of high O_3 in the lower free troposphere over the Pacific Northwest as observed at the Mt. Bachelor Observatory. *Atmos. Environ.* 45: 5302–5315.

Andreae, M.O. (1991). Biomass burning: Its history, use, and distribution and its impact on environmental quality and global climate, In *Global biomass burning: Atmospheric, climatic, and biospheric implications,* Levine, J.S. (Ed.), The MIT Press, Cambridge, MA, pp. 3–21

Andreae, M.O. and Merlet, P. (2001). Emission of trace gases and aerosols from biomass burning. *Global Biogeochem. Cycles* 15: 955–966.

Ångström, A.K. (1929). On the atmospheric transmission of Sun radiation and on dust in the air. *Geogr. Ann*. 11: 156–166.

Bange, H.W. and Williams, J. (2000). New directions: Acetonitrile in atmospheric and biogeochemical cycles. *Atmos. Environ*. 34: 4959–4960.

Bell, M.L., Peng, R.D. and Dominici, F. (2006). The exposure-response curve for ozone and risk of mortality and the adequacy of current ozone regulations. *Environ. Health Perspect.* 114: 523–536.

Bertschi, I.T. and Jaffe, D.A. (2005). Long-range transport of ozone, carbon monoxide and aerosols to the NE Pacific troposphere during the summer of 2003: Observations of smoke plumes from Asian boreal fires. *J. Geophys. Res.* 110: D05303.

Briggs, N.L., Jaffe, D.A., Gao, H., Hee, J.R., Baylon, P.M., Zhang, Q., Zhou, S., Collier, S.C., Sampson, P.D., and Cary, R.A. (2016). Particulate matter, ozone, and nitrogen species in aged wildfire plumes observed at the Mount Bachelor Observatory. *Aerosol Air Qual. Res.* 16: 3075–3087.

Crutzen, P.J. and Andreae, M.O. (1990). Biomass burning in the tropics: Impact on atmospheric chemistry and biogeochemical cycles. *Science* 250: 1669–1678.

Finlayson-Pitts, B.J. and Pitts, J.N. (1986). *Atmospheric Chemistry: Fundamentals and Experimental Techniques*, John Wiley and Sons, New York, NY.

Fiscus, E.L., Booker, F.L. and Burkey, K.O. (2005). Crop responses to ozone: uptake, modes of action, carbon assimilation and partitioning. *Plant Cell Environ.* 28: 997–1011.

Gratz, L.E., Jaffe, D.A. and Hee, J.R. (2015). Causes of increasing ozone and decreasing carbon monoxide in springtime at the Mt. Bachelor Observatory from 2004 to 2013. *Atmos. Environ.* 109: 323–330.

Henderson, B.H., Pinder, R.W., Crooks, J., Cohen, R.C., Carlton, A.G., Pye, H.O.T. and Vizuete, W. (2012). Combining Bayesian methods and aircraft observations to constrain the $HO^{\cdot} + NO_2$ reaction rate. *Atmos. Chem. Phys*. 12: 653–667.

Jacob, D. (1999). *Introduction to atmospheric chemistry*. Princeton University Press.

Jaffe, D.A., Anderson, T., Covert, D., Kotchenruther, R., Trost, B., Danielson, J., Simpson, W., Berntsen, T., Karlsdottir, S., Blake, D., Harris, J., Carmichael, G. and Uno, I. (1999). Transport of Asian air pollution to North America. *Geophys. Res. Lett.* 26: 711–714.

Jaffe, D., Bertschi, I., Jaegle´, L., Novelli, P., Reid, J.S., Tanimoto, H., Vingarzan, R. and Westphal, D.L. (2004). Long-range transport of Siberian biomass burning emissions and impact on surface ozone in western North America. *Geophys. Res. Lett*. 31: L16106.

Jaffe, D., Prestbo, E., Swartzendruber, P., Weiss-Penzias, P., Kato, S., Takami, A., Hatakeyama, S. and Kajii, Y. (2005). Export of atmospheric mercury from Asia. *Atmos. Environ.* 39: 3029–3038.

Jaffe, D. and Wigder, N. (2012). Ozone production from wildfires: A critical review. *Atmos. Environ.* 55: 1–10.

Kotchenruther R.A., Jaffe, D.A. and Jaeglé, L. (2001). Ozone photochemistry and the role of PAN in the springtime northeastern Pacific troposphere: Results from the PHOBEA campaign. *J. Geophys. Res.* 106: 731–741.

Laing, J.R., Jaffe, D.A. and Hee, J.R. (2016). Physical and optical properties of aged biomass burning aerosol from wildfires in Siberia and the Western USA at the Mt. Bachelor Observatory. *Atmos. Chem. Phys*. 16: 15185–15197.

Liang, Q., Jaegle, L., Jaffe, D.A., Weiss-Penzias, P., Heckman, A. and Snow, J.A. (2004). Long-range transport of Asian pollution to the northeast Pacific: Seasonal variations and transport pathways of carbon monoxide. *J. Geophys. Res.* 109: D23S07.

Martins, V., Miranda, A., Carvalho, A., Schaap, M., Borrego, C. and Sa, E. (2012). Impact of forest fires on particulate matter and ozone levels during the 2003, 2004 and 2005 fire seasons in Portugal. *Sci. Total Environ*. 414: 53–62.

Monks, P.S., Granier, C., Fuzzi, S., Stohl, A., Williams, M.L., Akimoto, H., Amann, M., Baklanov, A., Baltensperger, U., Bey, I., Blake, N., Blake, R.S., Carslaw, K., Cooper, O.R., Dentener, F., Fowler, D., Fragkou, E., Frost, G.J., Generoso, S., Ginoux, P., Grewe, V., Guenther, A., Hansson, H.C., Henne, S., Hjorth, J., Hofzumahaus, A., Huntrieser, H., Isaksen, I.S.A., Jenkin, M.E., Kaiser, J., Kanakidou, M., Klimont, Z., Kulmala, M., Laj, P., Lawrence, M.G., Lee, J.D., Liousse, C., Maione, M. and McFiggans, G. (2009). Atmospheric composition change – global and regional air quality. *Atmos. Environ*. 43: 5268–5350.

Palmer, P.I., Parrington, M., Lee, J.D., Lewis, A.C., Rickard, A.R., Bernath, P.F., Duck, T.J., Waugh, D.L., Tarasick, D.W., Andrews, S., Aruffo, E., Bailey, L.J., Barrett, E., Bauguitte, S.J.B., Curry, K.R., Di Carlo, P., Chisholm, L., Dan, L., Forster, G., Franklin, J.E., Gibson, M.D., Griffin, D., Helmig, D., Hopkins, J.R., Hopper,

J.T., Jenkin, M.E., Kindred, D., Kliever, J., Le Breton, M., Matthiesen, S., Maurice, M., Moller, S., Moore, D.P., Oram, D.E., O'Shea, S.J., Owen, R.C., Pagniello, C.M.L.S., Pawson, S., Percival, C.J., Pierce, J.R., Punjabi, S., Purvis, R.M., Remedios, J.J., Rotermund, K.M., Sakamoto, K.M., da Silva, A.M., Strawbridge, K.B., Strong, K., Taylor, J., Trigwell, R., Tereszchuk, K.A., Walker, K.A., Weaver, D., Whaley, C., and Young, J.C. (2013). Quantifying the impact of BO- Real forest fires on Tropospheric oxidants over the Atlantic using Aircraft and Satellites (BORTAS) experiment: Design, execution and science overview. *Atmos. Chem. Phys*. 13: 6239–6261.

Parrington, M., Palmer, P.I., Lewis, A.C., Lee, J.D., Rickard, A.R., Di Carlo, P., Taylor, J.W., Hopkins, J.R., Punjabi, S., Oram, D.E., Forster, G., Aruffo, E., Moller, S.J., Bauguitte, S.J.B., Allan, J.D., Coe, H. and Leigh, R.J. (2013). Ozone photochemistry in boreal biomass burning plumes. *Atmos. Chem. Phys*. 13: 7321–7341.

Reidmiller, D.R., Jaffe, D.A., Chand, D., Strode, S., Swartzendruber, P., Wolfe, G.M. and Thornton, J.A. (2009). Interannual variability of long-range transport as seen at the Mt. Bachelor Observatory. *Atmos. Chem. Phys*. 9: 557–572.

Seinfeld, J.H. and Pandis, S.N. (1998). *Atmospheric chemistry and physics*. Wiley-Interscience, New York, 1326 pp.

Teakles, A.D., So, R., Ainslie, B., Nissen, R., Schiller, C., Vingarzan, R., McKendry, I., Macdonald, A.M. and Jaffe, D.A. (2017). Impacts of the July 2012 Siberian fire plume on air quality in the Pacific Northwest. *Atmos. Chem. Phys*. 17: 2593–2611.

Zhang, L., Jacob, D.J., Boersma, K.F., Jaffe, D.A., Olson, J.R., Bowman, K.W., Worden, J.R., Thompson, A.M., Avery, M.A., Cohen, R.C., Dibb, J.E., Flock, F.M., Fuelberg, H.E., Huey, L.G., McMillan, W.W., Singh, H.B. and Weinheimer, A.J. (2008). Transpacific transport of ozone pollution and the effect of recent Asian emission increases on air quality in North America: An integrated analysis using satellite, aircraft, ozonesonde, and surface observations. *Atmos. Chem. Phys*. 8: 6117–6136.

Zhu, C., Kawamura, K., and Kunwar, B. (2015a). Effect of biomass burning over the western North Pacific Rim: Wintertime maxima of anhydrosugars in ambient aerosols from Okinawa. *Atmos. Chem. Phys*. 15: 1959–1973.

Zhu, C., Yoshikawa-Inoue, H., Tohjima, Y. and Irino, T. (2015b). Temporal variations in black carbon recorded on Rishiri Island, northern Japan. *Geochem. J.* 49: 283–294.

Received for review, June 23, 2017
Revised, September 4, 2017
Accepted, September 20, 2017